Integrating Intensity and Boundary Information for Tissue Classification

Dzung L. Pham
Laboratory of Medical Image Computing
Department of Radiology, Johns Hopkins University
Baltimore, MD 21287
E-mail: pham@jhu.edu

Abstract

A new algorithm is proposed for performing unsupervised tissue classification in medical images by integrating conventional clustering techniques with edge-adaptive segmentation techniques. Based on the fuzzy C-means algorithm, the algorithm computes a smooth segmentation while simultaneously estimating an edge field. Unlike most tissue classification algorithms that incorporate a smoothness constraint, the edge field estimation prevents the algorithm from smoothing across tissue boundaries, thereby producing robust yet accurate results. The algorithm is formulated as the minimization of an objective function that includes penalty terms to ensure that both the segmentation and edge field are relatively smooth.

1. Introduction

Tissue classification is a necessary step in many medical imaging applications such as the quantification of tissue volumes, the detection of pathology, and computer integrated surgery. Most tissue classification methods are based on clustering the pixel intensities within the image. These approaches are often made more robust by incorporating a spatial continuity constraint into the paradigm. The underlying assumption is that the resulting segmentation should favor large contiguous regions over small, disconnected regions.

A common method of incorporating spatial continuity into a segmentation algorithm is to employ a smoothness or Markov random field prior [1] that assumes that the neighbors of a pixel will likely belong to the same tissue class as the pixel itself. However, most tissue classification methods do not consider the fact that this assumption is violated when the pixel is adjacent to a tissue boundary. Because tissue boundaries appear as discontinuities in pixel intensity within the image, utilization of edge information can be used to prevent blurring across tissue boundaries. This approach has previously been used in image restoration [1], and surface reconstruction [2].

In [3], we described how edge-adaptive techniques can be incorporated into clustering-based tissue classification methods. Based on the fuzzy C-means (FCM) algorithm [4], a new algorithm was derived for performing tissue classification while simultaneously computing an edge field. In that work, the edge field was estimated on the same grid as the original image. The disadvantage of this approach is that estimated edges must be at least two pixels wide. In this work, we improve upon the previous approach by employing complementary grids for the edge field. The edge field is decomposed into separate components– horizontal and vertical in the two-dimensional (2-D) case– and allowed to exist between the original grid points. We provide results employing the new edge field formulation.

Proceedings of the 17th IEEE Symposium on Computer-Based Medical Systems (CBMS'04)
1063-7125/04 $ 20.00 © 2004 IEEE

2. Background

In [5] and [6], segmentation of two-dimensional magnetic resonance (MR) images was performed based on the minimization of the following energy functional with respect to the segmentation f, and the edge field s:

$$\int\int_{\Omega} \alpha(y-f)^2 + \beta(1-s)^2|\nabla f|^2 + \gamma(\rho|\nabla s|^2 + \frac{1}{\rho}s^2)\,dx\,dy \tag{1}$$

The above equation closely resembles the well-studied Mumford-Shah functional [5], except it uses a continuous edge penalty function rather than a binary one. In this equation, Ω is the domain of the image, y is the image data, and α, β, γ, and ρ are weighting parameters controlling the balance of each term. The edge field at each pixel will be a value between zero and one. The segmented image f, in this case is an approximation of y and will be piecewise smooth, as dictated by the second term that penalizes the gradient of y where edges are small. The third term penalizes both the existence of edges, as well as the gradient of the edge field. The effectiveness of equation (1) stems from the fact that the segmentation is not required to be smooth across edges, and because the edge field itself is constrained to be smooth.

Note that the *segmentation* obtained in the case of (1) differs significantly from what one would consider to be a *tissue classification*. The segmentation y is simply a partitioning of the image into an unrestricted number of contiguous regions, without any labels assigned to each region. On the other hand, a tissue classification typically has a fixed number of classes that are represented by potentially non-contiguous regions. Clustering-based tissue classification algorithms exploit the fact that the number of tissues are often known and that the intensity values of each class can be modeled by a parametric distribution. The estimated distributions can often be used to assign a label to each tissue class.

3. Methods

In this section, it is shown how the edge-adaptive properties of (1) can be incorporated into the fuzzy C-means clustering algorithm (FCM). Mathematically, FCM is derived by the minimizing the following objective function with respect to the membership functions u_{jk} and the centroids v_k:

$$J_{\mathrm{FCM}} = \sum_{j\in\Omega}\sum_{k=1}^{C} u_{jk}^{q}\|\mathbf{y}_j - \mathbf{v}_k\|^2 \tag{2}$$

where y_j is the observation at pixel j, C is the known number of clusters or classes, and Ω is the image domain. The membership functions are constrained to be positive and to satisfy

$$\sum_{k=1}^{C} u_{jk} = 1 \tag{3}$$

Here, the objective function is minimized when high membership values are obtained in areas where the observations are close to the centroid, and low membership values are obtained where observations are distant from the centroid. The parameter q is a weighting exponent that satisfies $q > 1$ and controls the degree of "fuzziness" in the resulting membership functions. As q approaches unity, the membership functions become more crisp, and approach binary functions. As q increases, the membership functions become increasingly fuzzy. For simplicity, the value of q is

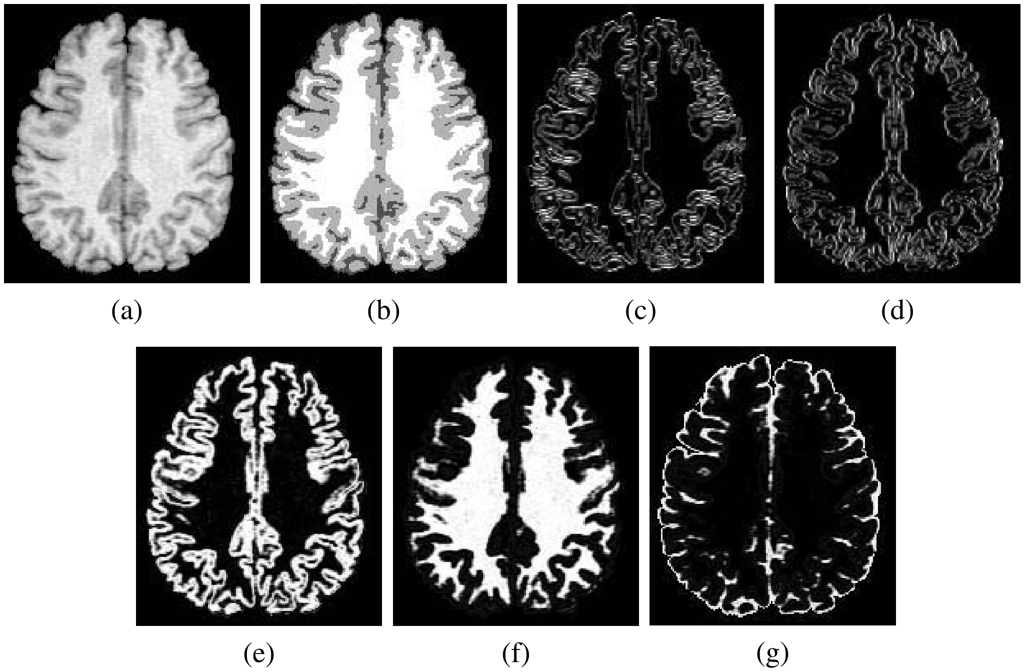

Figure 1: Results of applying edge-adaptive algorithm to a T1-weighted MR image: (a) MR image, (b) classification result using new algorithm, (c) horizontal edge field, (d) vertical edge field, (e)-(f) gray matter, white matter, and cerebrospinal fluid membership functions.

assumed to be 2, and $\mathbf{y}_j$ and $\mathbf{v}_k$ are assumed to be scalars y_j and v_k for the remainder of this paper. However, all of the following extends in a straightforward manner to the more general case.

For notational simplicity, we consider the 2-D case in the following, but the 3-D generalization is straightforward. The integrated tissue classification and boundary estimation algorithm can be formulated as the minimization of the following energy function:

$$\begin{aligned} J &= \alpha \sum_{j\in\Omega} \sum_{k=1}^{C} u_{jk}^2 \|y_j - v_k\|^2 \\ &+ \frac{\beta}{2} \sum_{j\in\Omega} \sum_{k=1}^{C} \sum_{m\neq k} \left(\sum_{l\in N_j^{(x)}} (1 - s_{j|l}^{(x)})^2 u_{jk}^2 u_{lm}^2 + \sum_{l\in N_j^{(y)}} (1 - s_{j|l}^{(y)})^2 u_{jk}^2 u_{lm}^2 \right) \\ &+ \frac{\gamma}{2} \sum_{j\in\Omega_x} \left(\frac{1}{\rho} (s_j^{(x)})^2 + \rho \sum_{l\in N_j} (s_j^{(x)} - s_l^{(x)})^2 \right) + \frac{\gamma}{2} \sum_{j\in\Omega_y} \left(\frac{1}{\rho} (s_j^{(y)})^2 + \rho \sum_{l\in N_j} (s_j^{(y)} - s_l^{(y)})^2 \right). \end{aligned} \tag{4}$$

Although Eq. 4 may appear complicated, it can be broken down into fairly simple parts. The first term is exactly the standard FCM objective functional, where Ω is the set of pixel locations, C is the number of clusters (assumed to be known), u are membership functions, y are the observed pixel values, and v are the cluster centroids or means. Without loss of generality, we consider only the case where the exponent on u, also called the "fuzzification parameter," is the commonly used value of 2.

The second line of Eq. 4 is a slight modification of the smoothness penalty on membership functions proposed in [7]. The main difference is that the penalty is modulated by horizontal and vertical edge fields, $s^{(x)}$ and $s^{(y)}$, which are allowed to vary between 0 and 1. We use the notation $N_j^{(x)}$ and $N_j^{(y)}$ to denote the set of horizontal and vertical neighbors of j, and $s_{j|l}$ to denote the edge value between pixel locations j and l. Thus, the membership functions are constrained to be smooth only across areas where the edge fields are small.

The third line of Eq. 4 consists of penalty functions on the horizontal and vertical edge fields to ensure that they are also smooth. This penalty function is the same as the edge penalty functions utilized in [2] except that the edge field has been decomposed into separate horizontal and vertical components. The complementary horizontal and vertical grids of the edge fields are denoted Ω_x and Ω_y, respectively. The parameters α, β, γ, and ρ control the relative balance of each term. For the edge field, γ controls the magnitude of each field while ρ controls the overall smoothness.

An iterative algorithm can be derived to minimize Eq. 4 by evaluating the centroids v_k, membership functions u_{jk}, and edge field s_j that satisfy a zero gradient condition. Because the second and third terms of (4) do not depend on v_k, the necessary conditions on the centroids for are identical to that of FCM [4]. A necessary condition on u_{jk} for J_{EAFCM} to be at a local minimum is

$$u_{jk} = \frac{\left(\alpha(y_j - v_k)^2 + \beta(\sum_{l \in N_j^{(x)}} (1 - s_{j|l}^{(x)})^2 \sum_{m \neq k} u_{lm}^2 + \sum_{l \in N_j^{(y)}} (1 - s_{j|l}^{(y)})^2 \sum_{m \neq k} u_{lm}^2)\right)^{-1}}{\sum_{i=1}^{C} \left(\alpha(y_j - v_i)^2 + \beta(\sum_{l \in N_j^{(x)}} (1 - s_{j|l}^{(x)})^2 \sum_{m \neq k} u_{lm}^2 + \sum_{l \in N_j^{(y)}} (1 - s_{j|l}^{(y)})^2 \sum_{m \neq k} u_{lm}^2)\right)^{-1}} \tag{5}$$

A necessary condition on $s_j^{(x)}$ for (4) to be minimized is that $s_j^{(x)}$ must satisfy

$$\sum_{l,n} \sum_{k=1}^{C} \sum_{m \neq k} u_{nk}^2 u_{lm}^2 = (\sum_{l,n} \sum_{k=1}^{C} \sum_{m \neq k} u_{nk}^2 u_{lm}^2 + \frac{\gamma}{\rho\beta}) s_j^{(x)} + \frac{\gamma\rho}{\beta} \nabla^2 s_j^{(x)} \tag{6}$$

where the summation over l,n are indices referring to membership values on opposite sides of j in the x direction on the image grid. Equation (6) is a difference equation with spatially varying coefficients. In fact, it is of the same form as the gain field equations of [8] and can be solved efficiently using a multigrid algorithm. The necessary condition for $s_j^{(y)}$ is analogous to (6) and must also be computed. Iteration through these necessary conditions results in an algorithm for minimizing the objective function J.

4. Results

Figure 1 shows the results of applying the algorithm to a single slice of a T_1-weighted magnetic resonance brain image. Fig. 1a shows the original image. Fig. 1b shows the hard segmentation computed by assigning each pixel to the class of highest membership. Figs. 1c-d show the horizontal and vertical edge fields. It is apparent that the edge structure within the image, particular around the cortex of the brain, is primarily diagonal. This results in both vertical and horizontal edges being estimated. Figs. 1e-g show the membership functions corresponding to gray matter, white matter, and cerebrospinal fluid in the brain. The membership functions are fairly smooth but still reveal much of the detailed structure within the brain.

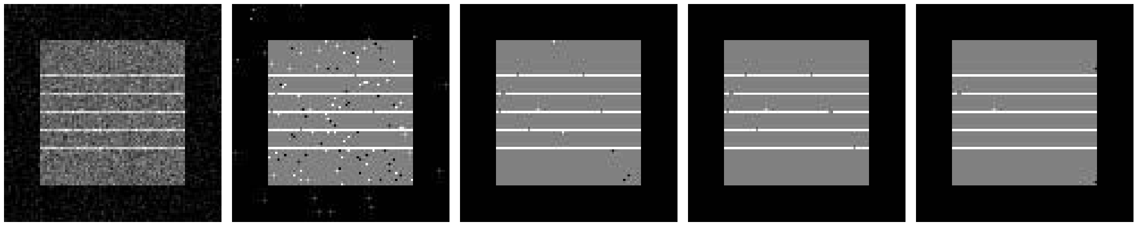

(a) (b) (c) (d) (e)

Figure 2: Illustration of edge fields: (a) input image, (b) FCM classification result, (c) FCM with smoothing result, (d) FCM with edge-adaptive smoothing result, (e) FCM with complementary grid edge-adaptive smoothing result.

Fig. 2a shows a synthetic three-class image with additive Gaussian noise. Figs. 2b-e show the classifcation results of applying standard FCM, FCM with just the smoothing penalty (equivalent to the case where $\gamma = 0$), the original edge-adaptive algorithm, and the new edge-adaptive algorithm using complementary grids for the edges, respectively. Parameters were selected empirically to maximize performance. The new algorithm has the ability to recover breaks in the stripes because it is capable of smoothing along the thin stripe, unlike the previous edge-adaptive algorithm.

5. Discussion

We have presented a tissue classification algorithm that incorporates boundary-adaptive smoothness constraints. Because the edges are computed on complementary grids, fine details within an image are preserved while homogeneous but noisy regions generate smooth classifications. Additional validation results on three-dimensional medical images are required to further quantify the performance of the approach. The use of complementary grids is somewhat limited when segmenting structures that have diagonal structure since this will prevent smoothing in both the horizontal and vertical directions.

References

[1] S. Geman and D. Geman. Stochastic relaxation, Gibbs distributions, and the Bayesian restoration of images. *IEEE Trans. on Pattern Anal. Machine Intell.*, PAMI-6:721–741, 1984.

[2] J.M. Gauch J. Shah, H.H. Pien. Recovery of surfaces with discontinuities by fusing shaing and range data within a variational framework. *IEEE Trans. on Image Processing*, 5(8):1243–1251, 1996.

[3] D.L. Pham. Unsupervised tissue classification in medical images using edge-adaptive clustering. In *Proceedings of the 25th International Conference of the IEEE Engineering in Medicine*, Cancun, Mexico, 2003.

[4] J.C. Bezdek. A convergence theorem for the fuzzy ISODATA clustering algorithms. *IEEE Trans. on Pattern Anal. Machine Intell.*, PAMI-2, 1980.

[5] H.H. Pien and J.M. Gauch. Variational segmentation of multi-channel MRI images. In *Proceedings of the 1994 IEEE International Conference on Image Processing*, volume 3, pages 508–512, 1994.

[6] J. Kaufhold, M. Schneider, A.S. Willsky, and W.C. Karl. A statistical method for efficient segmentation of MR imagery. *Internation Journal of Pattern Recognition and Artificial Intelligence*, 11(8):1213–1231, 1997.

[7] D.L. Pham. Spatial models for fuzzy clustering. *Computer Vision and Image Understanding*, 84(2):285–297, 2001.

[8] D.L. Pham and J.L. Prince. Adaptive fuzzy segmentation of magnetic resonance images. *IEEE Trans. on Medical Imaging*, 18(9):737–752, 1999.

Proceedings of the 17th IEEE Symposium on Computer-Based Medical Systems (CBMS'04)